

Research article

# Application of polydimethylsiloxane (PDMS) as a flexible substrate for wireless body and local area network antenna with CSRR integration

Praveen Kumar Sharma<sup>1\*</sup>, Jae-Young Chung<sup>2</sup>

<sup>1</sup>Research Center for Electrical and Information Technology, Seoul National University of Science and Technology, 01811 Seoul, Republic of Korea

<sup>2</sup>Department of Electrical and Information Engineering, Seoul National University of Science and Technology, 01811 Seoul, Republic of Korea

Received 31 January 2023; accepted in revised form 3 April 2023

**Abstract.** This research illustrates the application of PDMS (polydimethylsiloxane), a silicon-based polymer with loss tangent ( $\tan \delta_{ep}$ ) and dielectric constant ( $\epsilon_r$ ) values of 0.02 and 2.65, as a flexible substrate for antenna (PDMS substrate based flexible antenna – PSFA). In this paper, two flexible antennas having a size of  $50.2 \times 40.1 \times 1$  mm are presented for wireless body and local area networks. A split ring resonator (CSRR) structure with circular geometry is integrated on the patch in the second proposed antenna as compared to the first antenna with the same dimensions. As a result, this antenna has multiband notched frequency characteristics at 5.12, 5.80, and 6.66 GHz, respectively, with improved performance. It also helped to reduce SAR and backward radiation. Both of the proposed antennas behave well and exhibit significant concordance between simulation and measurement findings when tested in various operational situations, including wet and conformal conditions and demonstrate the suitability of PDMS as a flexible substrate for antenna applications.

**Keywords:** *adhesion, conformal analysis, flexible antenna, modeling and simulation, material testing, PDMS*

## 1. Introduction

Compared to conventional electronic devices with rigid substrates, flexible substrate-based electronics have many benefits. These flexible devices can withstand unusual operating environments like twisting, bending, and stretching. As a result of additional atypical performance requirements brought on by the rising demand for novel wireless communication systems in recent years, antenna designers have had to overcome a number of technological impediments. For such applications, it is preferable to have a flexible, compact, lightweight, easily integrable, and inexpensive antenna. These qualities are also desired in wearable antennas [1] for body-worn applications because they mitigate potential health risks

for the user. As a result, flexible antennas designed utilizing flexible substrates are preferred over traditional antennas using rigid substrates to satisfy such requirements.

Materials for conductive portions like patch, ground, and feed, as well as substrate materials, should be carefully chosen when designing a flexible antenna. This decision will largely depend on the desired applications taken into account. Fabric, polymers, and paper-based substrates are the three basic categories of flexible substrates that may be utilized to develop flexible antennas. The vulnerability of fabric substrates to external factors like temperature variations and hydrophilicity is higher. They perform only partially when conditions are flexible, stretchable, and

\*Corresponding author, e-mail: [impraveenkumarsharma@gmail.com](mailto:impraveenkumarsharma@gmail.com)  
© BME-PT

conformal [2]. Similar restrictions apply to paper-based substrates; hence polymer-based substrate polydimethylsiloxane (PDMS) is favored in this research.

Researchers are always experimenting with new approaches and materials to enhance the performance of flexible and wearable antennas. One is the use of metamaterial loading in flexible and wearable antennas. Flexible antennas' performance can be further enhanced by various metamaterial structures, such as split-ring resonators (SRRs), by downsizing their size, boosting their bandwidth, efficiency, and directivity, and enhancing their radiation patterns [3, 4]. These features facilitate wave polarization, wave absorption, and surface wave reduction. For lowering the specific absorption rate (SAR) of flexible/wearable antennas, metamaterial surfaces have also gained popularity. By reducing the energy the body absorbs, metamaterials are frequently employed to protect the human body from dangerous radiation [5]. They are unquestionably helpful in antenna design. Still, a great deal of research is to be done in this field, particularly their implementation in flexible and wearable antennas using polymer substrates like PDMS. This encouraged us to design and analyze a PDMS substrate-based flexible antenna-2 (PSFA-2) for wireless body and local area networks that is inspired by a split ring resonator (CSRR) structure and compare it to a flexible antenna having the same dimensions (PSFA-1) that is not loaded with CSRR to assess its advantages. There are several pieces of research available in the literature that employs SRRs in the antenna design to create frequency notches and broadband behavior and to improve the antenna performance. Still, there are very few on the design of flexible/wearable antennas with CSRR loading, particularly using the polymer substrates like polydimethylsiloxane (PDMS) for the targeted wireless local area network (WLAN) and wireless body area network (WBAN) applications as presented in this paper. Furthermore, many researchers have employed a variety of CSRRs and their arrays, but here only one CSRR employed in PSFA-2 is performing the same task, thus reducing the design complexity. The employed substrate PDMS in both of the presented antennas is fabricated and characterized to improve the design accuracy and both of the presented antennas are tested under varying operating conditions. Simple antenna structures, even with the CSRR incorporation, stable and enhanced performance with

flexibility, easy and cost-effective development process make the proposed antennas employable, and PDMS a good candidate as a flexible substrate for the targeted applications; these are some of the major contributions of the presented research as compared to the previous works.

Both of the proposed antennas show a multiband behavior and operate at the 5.0 GHz band (Institute of Electrical and Electronics Engineers, IEEE 802.11ac) to resolve the 2.45 GHz band's issues relating to traffic and the 6.0 GHz (IEEE 802.11ax) band, which was just debuted in 2020 for fast wireless local area network applications. To address fast wireless body area network applications, an additional band of 5.8 GHz (IEEE 802.16d) is attained in the PSFA-2 by a single CSRR loading. The presented paper is divided into five sections. After a brief introduction in section 1, section 2 provides an overview of the PDMS development and characterization techniques. Antenna designs and fabricated prototypes are presented in section 3. In section 4, the performance of both the presented PSFAs is compared with SAR, conformal, and wet condition analysis. Finally, the paper is concluded in section 5 by summarizing all the results obtained.

## 2. PDMS Fabrication and dielectric characterization

The choice of substrate is a crucial component of antenna design since its physical and dielectric qualities have a direct impact on the antenna's radiating properties. Polydimethylsiloxane (PDMS), which is a silicone-based elastomer belonging to silicon-organic compounds, is used as a flexible substrate in both of the proposed antennas. PDMS has gained popularity in recent years not only as a substrate for antenna applications but also as a coating for antenna hydrophobics [6], wearable sensors [7], membranes [8], *etc.* It possesses qualities that make it an appropriate substrate for flexible antennas – it is highly flexible (Young's modulus <3 MPa) and transparent, has less effect of environmental variations like absorption of moisture, is thermally and chemically stable, and has nearly isotropic dielectric properties [9]. The flexible substrate PDMS is developed using the conventional process, as summarized in Figure 1. After the substrate has been chosen and successfully developed in accordance with the specifications, its characterization is carried out utilizing our prior research [10–12]. Since PDMS is anisotropic, the values

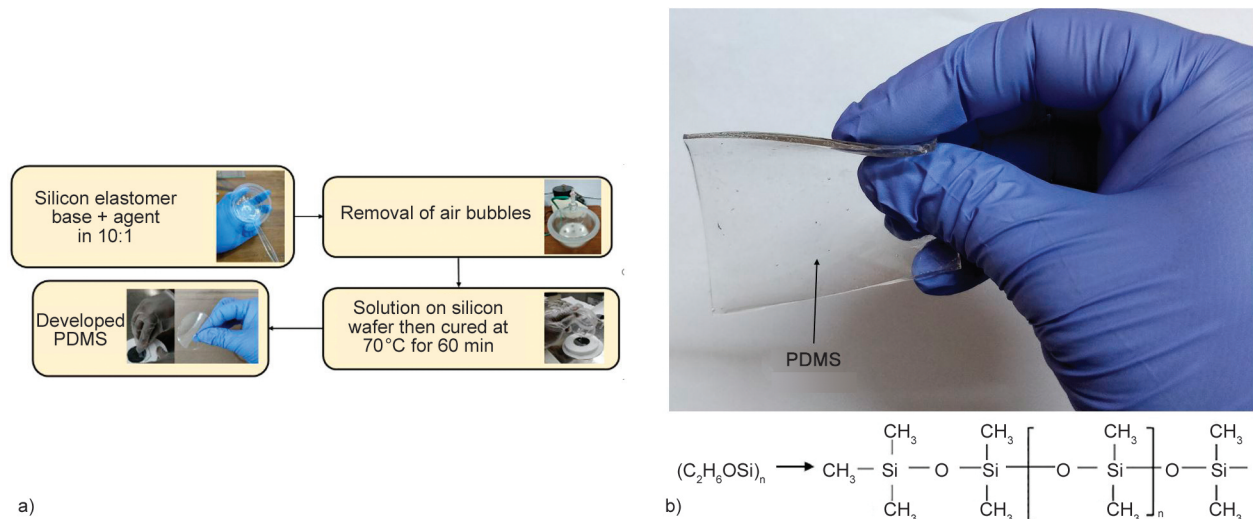


Figure 1. a) PDMS development process, and b) developed PDMS.

for the dielectric properties vary in different directions. The characterization of the PDMS as a flexible substrate is crucial since it has been noted from the literature that various researchers have employed different values of the dielectric characteristics for various applications [13–15]. This variation in the values of the dielectric parameters is mainly because of the applied characterization methods like, for example, conventional methods like Kent, free-space, Courtney, *etc.*, methods evaluate the dielectric parameters in a parallel direction [16–18]. Whereas the methods like transverse magnetic (TM) mode, re-entrant cavity, substrate integrated waveguide (SIW), *etc.* methods investigate the dielectric parameters in a perpendicular direction [19–21]. All of these methods are not appropriate for the characterization of polymers and may result in variable outcomes for anisotropic substrates.

Resonance and planar structure techniques based on our past works are employed here to investigate the PDMS dielectric characteristics [9, 10]. As shown in Figure 2a, two distinct resonators, R1 (for parallel values) and R2 (for perpendicular values), were

designed exclusively for resonance measurements of PDMS’s dielectric characteristics in both directions. The measurements show that the dielectric constants were 2.7 and 2.5, and the loss tangents were 0.03 and 0.02 in parallel and perpendicular directions, respectively. Therefore, it should be underlined that the perpendicular dielectric constant is approximately 5.1% smaller than the parallel one, demonstrating the low anisotropy of this material.

This method is also applied to other similar materials to validate the acquired values, and when their resulting values are compared with the values provided by the manufacturer, a reasonable correlation is found, as shown in Table 1. The covered ring resonator, shown in Figure 2b, has been used in planar structure measurements to assess the isotropic counterparts to PDMS’s anisotropic dielectric characteristics and help to minimize simulation problems with the anisotropic substrates in antenna applications. The loss tangent is calculated to be 0.02, and the dielectric constant to be 2.65. The isotropic equivalent values of the PDMS lie between the parallel-perpendicular values, as illustrated in Figure 3.

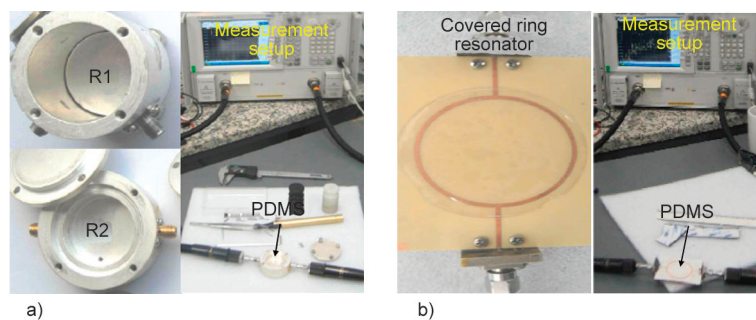
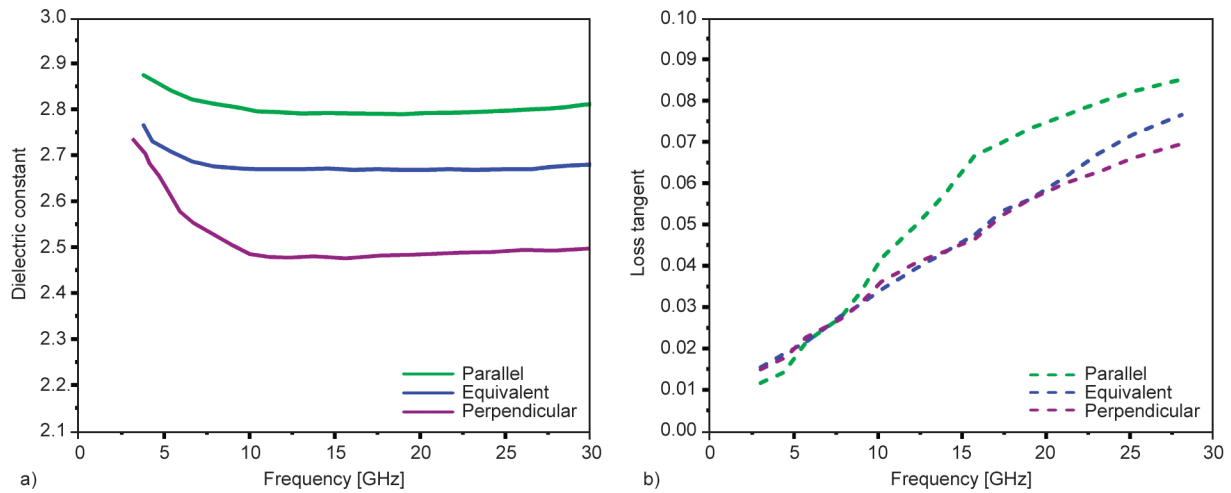


Figure 2. Measurement setups for a) Resonance measurement, and b) planar structure measurement method.

**Table 1.** Dielectric values of different materials by the resonance measurements (approximates).

Material	Perpendicular value, $\frac{\tan \delta_{\epsilon_r \text{perpendicular}}}{\epsilon_{r \text{perpendicular}}}$ (~)	Parallel value, $\frac{\tan \delta_{\epsilon_r \text{parallel}}}{\epsilon_{r \text{parallel}}}$ (~)
Polydimethylsiloxane (PDMS)	0.0200/2.5	0.0300/2.7
Cyclic olefin copolymer (COP)	0.0003/2.3	0.0005/2.3
Polytetrafluoroethylene (PTFE)	0.0002/2.0	0.0003/2.1
Polycarbonate (PC)	0.0050/2.7	0.0060/2.7



**Figure 3.** Obtained dielectric values by resonance and planar measurements: a) dielectric constant values and b) loss tangent values.

### 3. Antenna design

Two flexible antennas (PSFA-1 and 2) for wireless body and local area networks are presented in this paper. The PSFA-2 incorporates a CSRR structure to exemplify the advantages of employing it in flexible antenna designs with PDMS substrate; however, both antennas have the same physical dimensions.

#### 3.1. Antenna geometry

Both of the proposed flexible antennas of size  $50.2 \times 40.1 \times 1$  mm having a circular patch are designed using PDMS as a flexible substrate with  $\epsilon_r$  of 2.65 and  $\tan \delta_{\epsilon_r}$  of 0.02. The antenna geometries are depicted in Figure 4 and listed in Table 2 with their precise dimensions. In order to examine the effects

**Table 2.** Antenna physical parameters.

Parameter	$l$	$w$	$r$	$f_i$	$f_w$	$g_l$	$g_w$	$l_g$	$w_g$	$l_s$	$w_s$
	[mm]										
Value	50.2	40.1	15.0	17.0	18.0	19.0	3.0	50.2	40.1	12.0	0.5

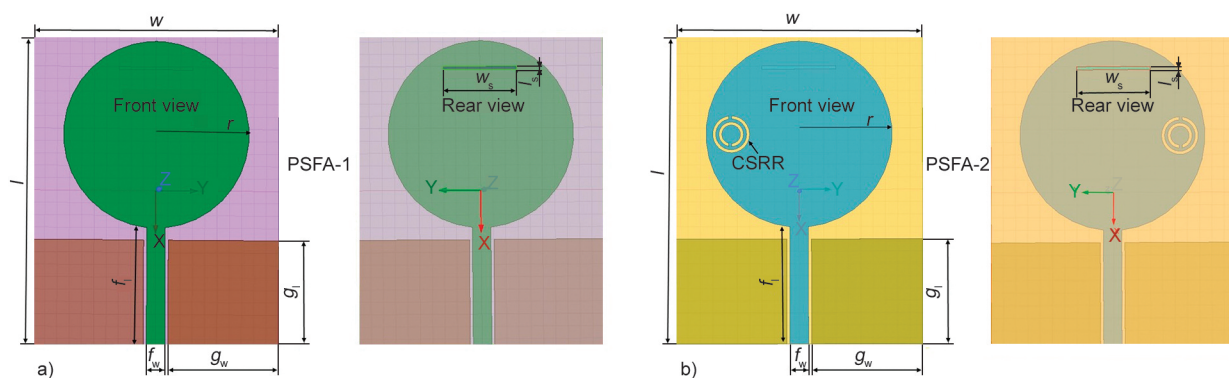


**Figure 4.** Antenna geometries: a) PSFA-1, and b) PSFA-2.

on the radiation performance, which are detailed in later portions of this paper, a CSRR structure is inserted in the PSFA-2 on the same side of the patch. Prior to being used in the antenna design, the CSRR is additionally examined and optimized for its behavior [22] using Ansys HFSS software.

The incorporation of the CSRR in the antenna design is quite advantageous since it makes the design more compact while acting as a magnetic resonator, increases bandwidth by limiting standing waves, and enhances the antenna’s radiation characteristics. These benefits are experimentally confirmed in the later sections of this paper in the design and analysis of PSFA-2.

The circular SRR's resonant frequency ( $f_{res}$ ) is (Equation (1)):

$$f_{res-CSRR} = \frac{1}{2\pi} \sqrt{\frac{1}{L_{total}C_{total}}} = \frac{1}{2\pi \sqrt{L_{total} \left[ \frac{(\pi r_{avg} - s_{gap})C_{pul}}{2} + \frac{\epsilon_0 \omega l}{2s_{gap}} \right]}} \quad (1)$$

where  $L_{total}$  and  $C_{total}$  are the total inductance and total capacitance of the unit cell structure,  $r_{avg}$  is the

ring’s average radius,  $s_{gap}$  is the gap in split,  $C_{pul}$  is the per unit length capacitance. The total inductance of the unit cell is (Equation (2)):

$$L_{total} = 0.0002l_w \left( 2.303 \log_{10} \frac{4l_w}{t} - c \right) \mu H \quad (2)$$

where  $l_w$  is the wire’s cross-section length for a single loop,  $c$  is the wire loop geometry constant, and is equal to 2.4.

The CSRR unit cell geometry is shown in Figure 5a, and the equivalent circuits of both PSFAs are depicted in Figure 5b and Figure 5c, respectively. Its response as an SRR structure is confirmed by Figure 6, which shows that the SRR has a negative permeability and permittivity in the required region of operation. The CSRR interacts dynamically with electromagnetic waves when these parameters are negative, as it produces a negative refractive index, which lessens standing waves and enhances the antenna’s performance.

### 3.2. Fabrication of prototypes

The prototypes of the presented antennas are developed and measured using the vector network analyzer

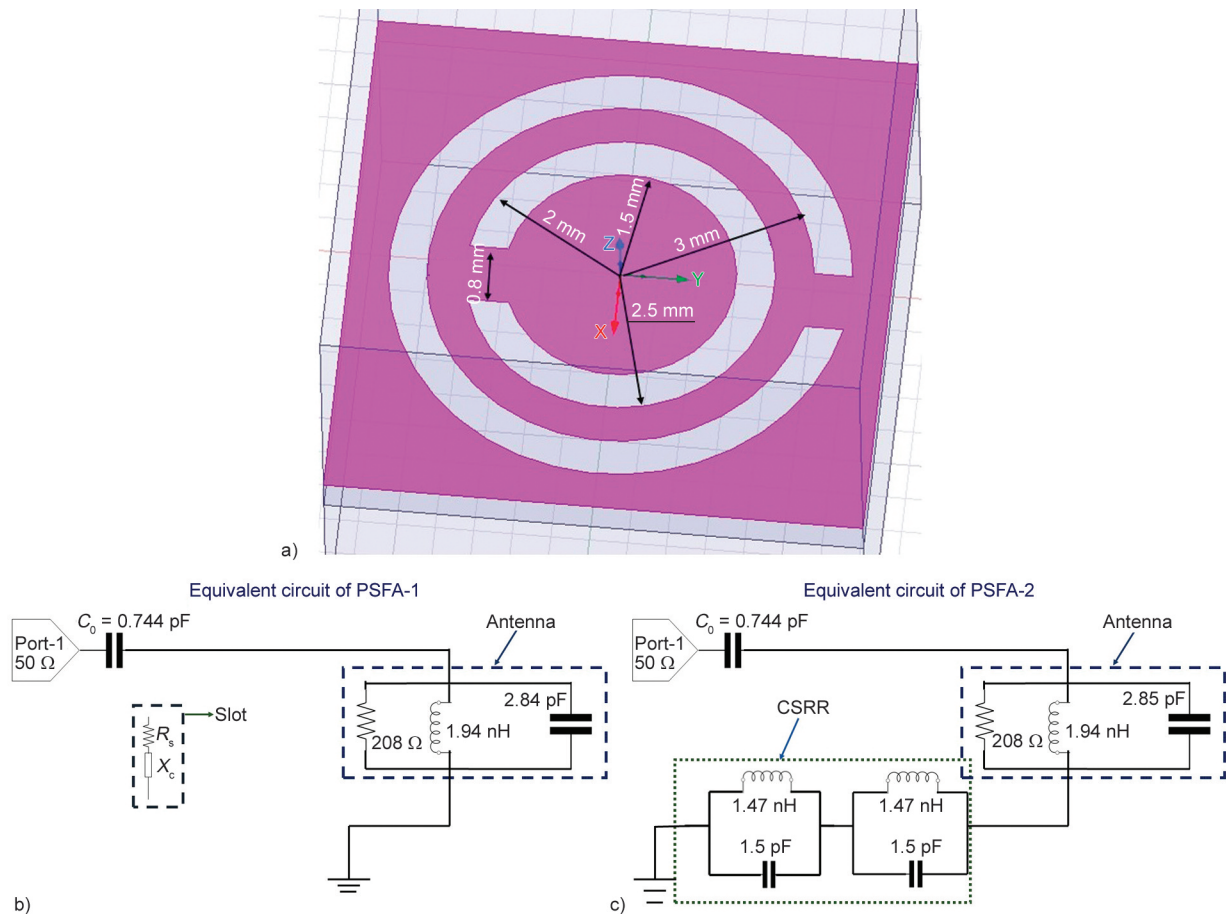


Figure 5. a) Circular SRR dimensions; equivalent circuits: b) PSFA-1, and c) PSFA-2.

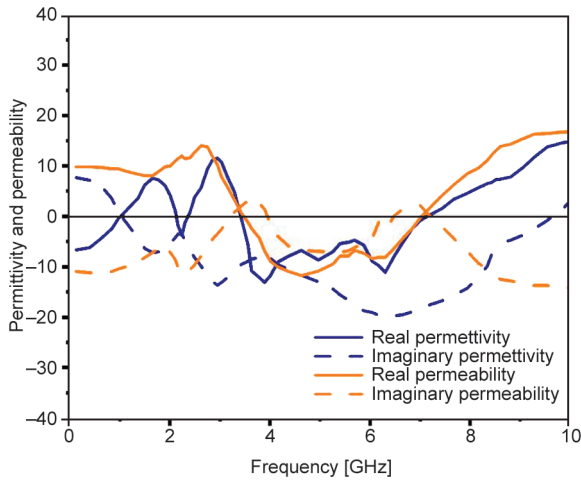


Figure 6. Circular SRR response.

(VNA) Figure 7, to validate the simulation results. In order to fabricate the antennas, first of all, the PDMS is developed as mentioned in section 2 with the required thickness of 1 mm, then it is cut as per the antenna dimensions of 50.2×40.1 mm. The copper tape 0.059 mm thick is used for the metallic parts of the antenna. Due to its superior adhesive qualities, the flexible substrate PDMS makes it simple for the copper tape to adhere. Both fabricated antennas exhibit steady performance even under variable working conditions, as described in the following sections of this article.

#### 4. Performance analysis

The evaluation of the obtained results from the simulation and measurement of the two designed PSFAs is carried out in this section. Both antennas are compared while operating under varying operating situations like conformal and wet conditions with SAR analysis.

#### 4.1. Radiation parameters

Both of the presented antennas show notched frequency behavior for the target applications, as shown in Figure 8. The PSFA-1 with dual-band behavior has impedance bandwidths of 0.75 GHz (4.60–5.35 GHz) at 5.03 and 0.51 GHz (6.39–6.90 GHz) at 6.53 GHz; 0.698 GHz (5.00–5.69 GHz) at 5.40 and 0.5 GHz (6.10–6.60 GHz) at 6.70 GHz in the simulation and experimental results respectively. While the PSFA-2 shows a triple band behavior having impedance bandwidths of 0.83 GHz (4.50–5.33 GHz) at 5.12 GHz, 0.64 GHz (5.60–6.24 GHz) at 5.80 GHz, and 0.53 GHz (6.35–6.88 GHz) at 6.66 GHz in simulation and 0.8 GHz (4.80–5.60 GHz) at 5.24, 0.61 GHz (5.62–6.23 GHz) at 5.72 and 0.518 GHz (6.48–6.99 GHz) at 6.81 GHz in measured results respectively. Figure 9 illustrates the voltage standing wave ratio (*VSWR*) of both the presented antennas with both simulation and measurement results having values less than 2. The close correlation between the simulation and measured radiation patterns at resonating frequencies across different planes is illustrated in the Figure 10 and Figure 11. Both of the proposed PSFAs exhibit nearly omnidirectional radiation patterns and show a conventional monopole behavior. The total gain of the PSFA-1 and PSFA-2 is 4.8 and 6.3 dBi, respectively (Figure 12). The third frequency band at 5.8 GHz, a decrease in the reflection coefficient ( $S_{11}$ ) and *VSWR*, and an enhancement in antenna gain can all be vividly viewed from the discussions above as benefits of implementing a single CSRR in the PSFA-2 with polymer substrate PDMS as summarized in Table 3. *E*-field distribution of both PSFAs are shown in Figure 13.

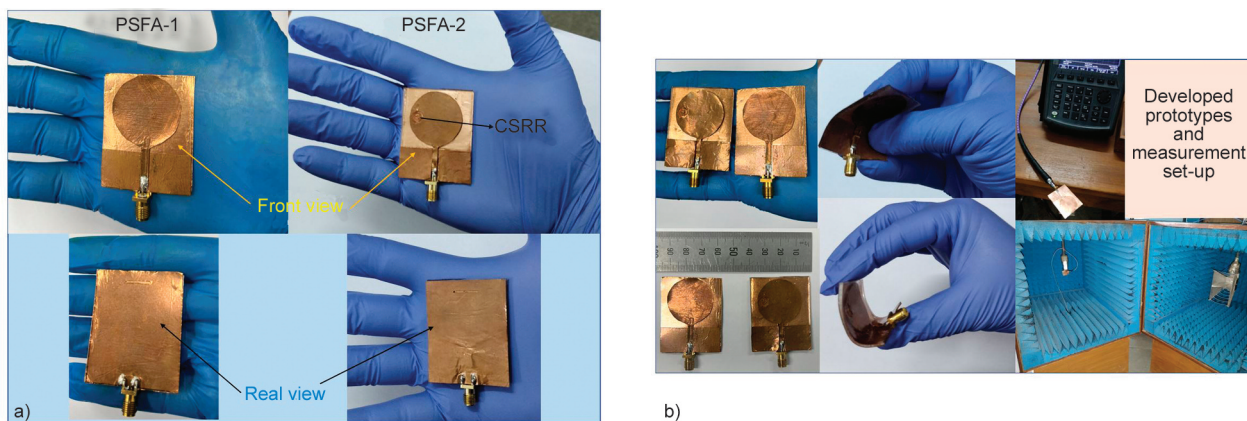


Figure 7. Fabricated prototypes: a) PSFA-1 and PSFA-2, and b) prototypes and measurements.

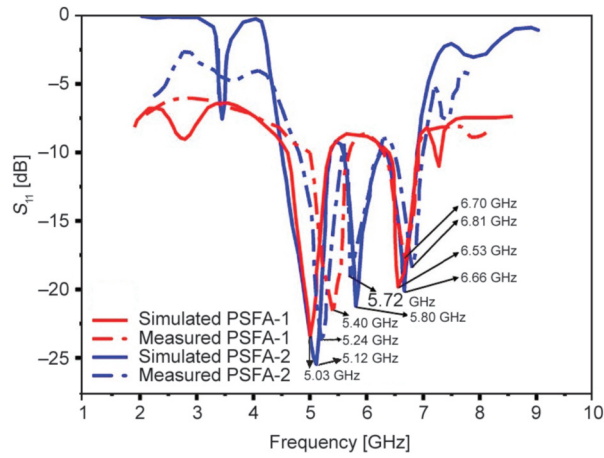


Figure 8.  $S_{11}$  values for the PSFAs (1 and 2).

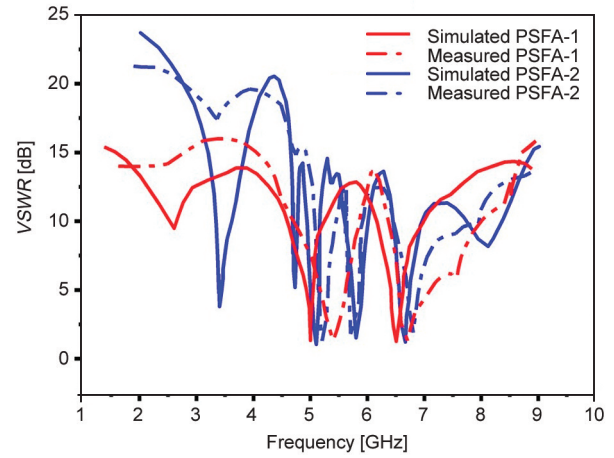


Figure 9.  $VSWR$  values for the PSFAs (1 and 2).

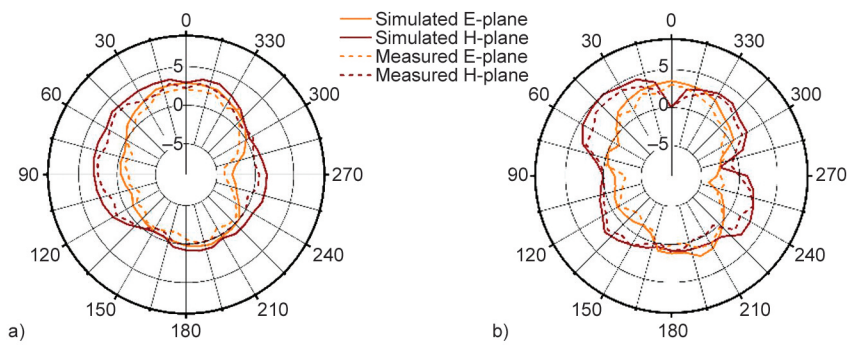


Figure 10. PSFA-1 radiation patterns, a) 5.0 GHz, b) 6.5 GHz.

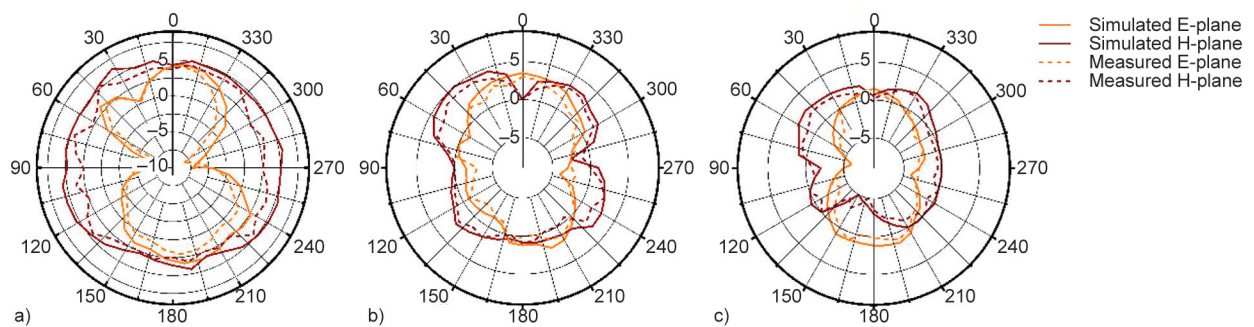


Figure 11. PSFA-2 radiation patterns, a) 5.10 GHz, b) 5.80 GHz, c) 6.60 GHz.

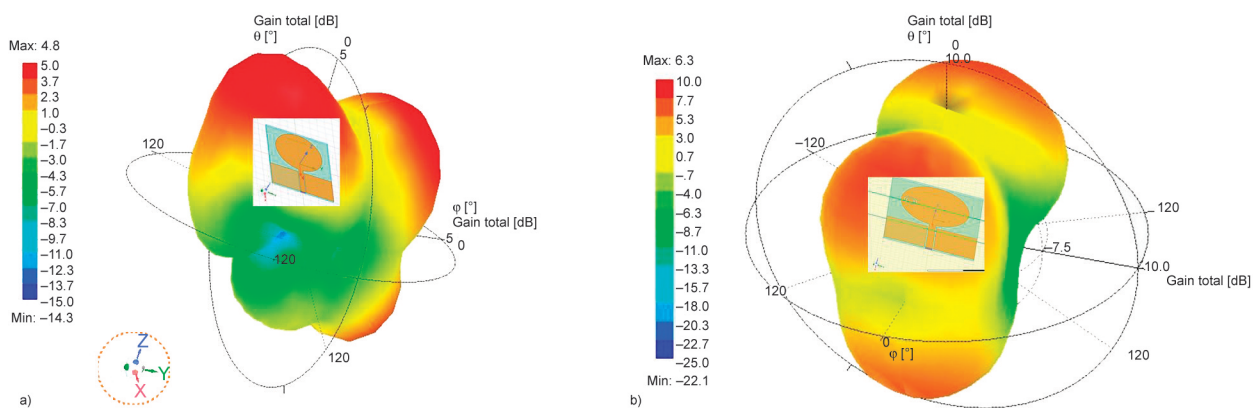
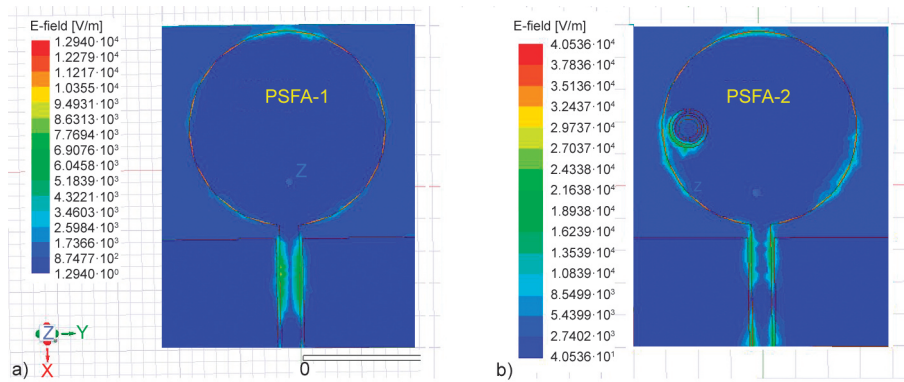


Figure 12. 3D gain plot: a) PSFA-1, and b) PSFA-2.

**Table 3.** Comparison of PSFAs.

Parameters	PSFA-1				PSFA-2					
	Simulation results		Experimental results		Simulation results			Experimental results		
Frequency [GHz]	5.03	6.53	5.40	6.70	5.12	5.80	6.66	5.24	5.72	6.81
$S_{11}/VSWR$ [dB]	-23.4/1.32	-19.8/1.26	-21.8/1.56	-18.1/1.32	-25.6/1.02	-21.2/1.50	-20.1/1.20	-24.0/1.30	-19.1/1.80	-18.4/1.92
-10 dB BW [GHz]	0.75	0.51	0.69	0.50	0.83	0.64	0.53	0.80	0.61	0.51
Gain [dBi]	4.0	1.8	3.8	1.5	6.2	4.1	2.4	6.0	4.2	2.2



**Figure 13.** E-field distribution for the a) PSFA-1 and b) PSFA-2.

#### 4.2. Estimation of SAR using simulation model

Employing a multi-layered model in simulation (Figure 14a), the specific absorption rate (SAR) analysis is carried out to examine how the proposed antennas affect the human body. The bottom layer of the SAR analysis model represents muscle, the mesoderm layer is fat, and the top is the skin [5, 23]. The

obtained SAR values (averaged) by this model for PSFA-1 (5.03 GHz) and PSFA-2 (5.12 GHz) using an input power of 100 mW are shown in Figure 14b and Figure 14c. The measured values are 1.9 and 1.6 W/kg, respectively, which satisfy the European standard (<2 W/kg). Thus, in the second proposed antenna, the CSRR with PDMS substrate aided in reducing the SAR also.

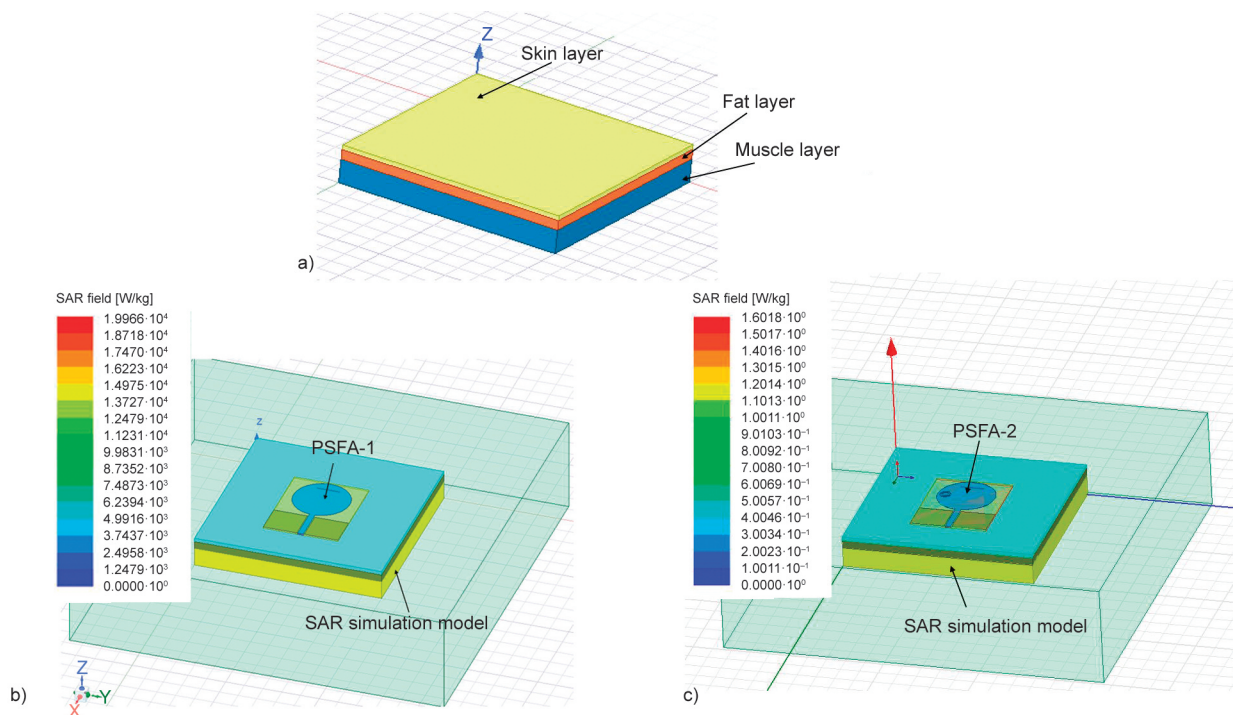


**Figure 14.** SAR Estimation: a) simulation model, b) for PSFA-1, and c) for PSFA-2.

### 4.3. Conformal condition analysis

The adoption of PDMS as a substrate has offered proposed antennas considerable flexibility so that they can be employed in conformal environments. Therefore in this sub-section, the developed antennas are evaluated under conformal conditions to assess their effects on the performance. Two different scenarios are chosen to observe its effects: firstly, the performance of both the antennas is tested on a hand at a  $\sim 10^\circ$  bent, and in the second, measurements are made using two different cylinders with radii of 3 and 4 cm. When adopted for wearable applications, one of the essential considerations of the flexible antenna should function effectively while mounted on the body, in contrast to the constraint of stiff substrate antennas. Due to the presence of biological tissues that might drain some power, it behaves as a lossy medium. This drives the S-parameters of the presented antennas to fluctuate (Figure 15a), and changes in the resonating frequencies can also be noticed. It is noteworthy that the given antennas retain

operation in the relevant frequency bands and possesses multiband capabilities. The dielectric characteristics of the substrate are crucial in this situation. Considering that PDMS has a comparatively low dielectric constant, it aids in suppressing surface waves and helps in achieving good impedance matching.

Both antennas are placed on cylinders with radii of 4.0 and 3.0 cm to investigate further the impact of bending on the antennas' radiating properties. Resonant frequencies and associated  $S_{11}$  values demonstrate a minor shift. However, as seen in Figure 15b and Figure 15c, the antennas still work in the needed multi-frequency bands while offering the notched features. Since PDMS is a substantially anisotropic substrate [9–12], it has been demonstrated experimentally and analytically that anisotropy and bending have opposing effects on the antenna's resonant properties [24, 25]. The results of the experimental investigation carried out here, and earlier studies are in satisfactory correlation with one another.

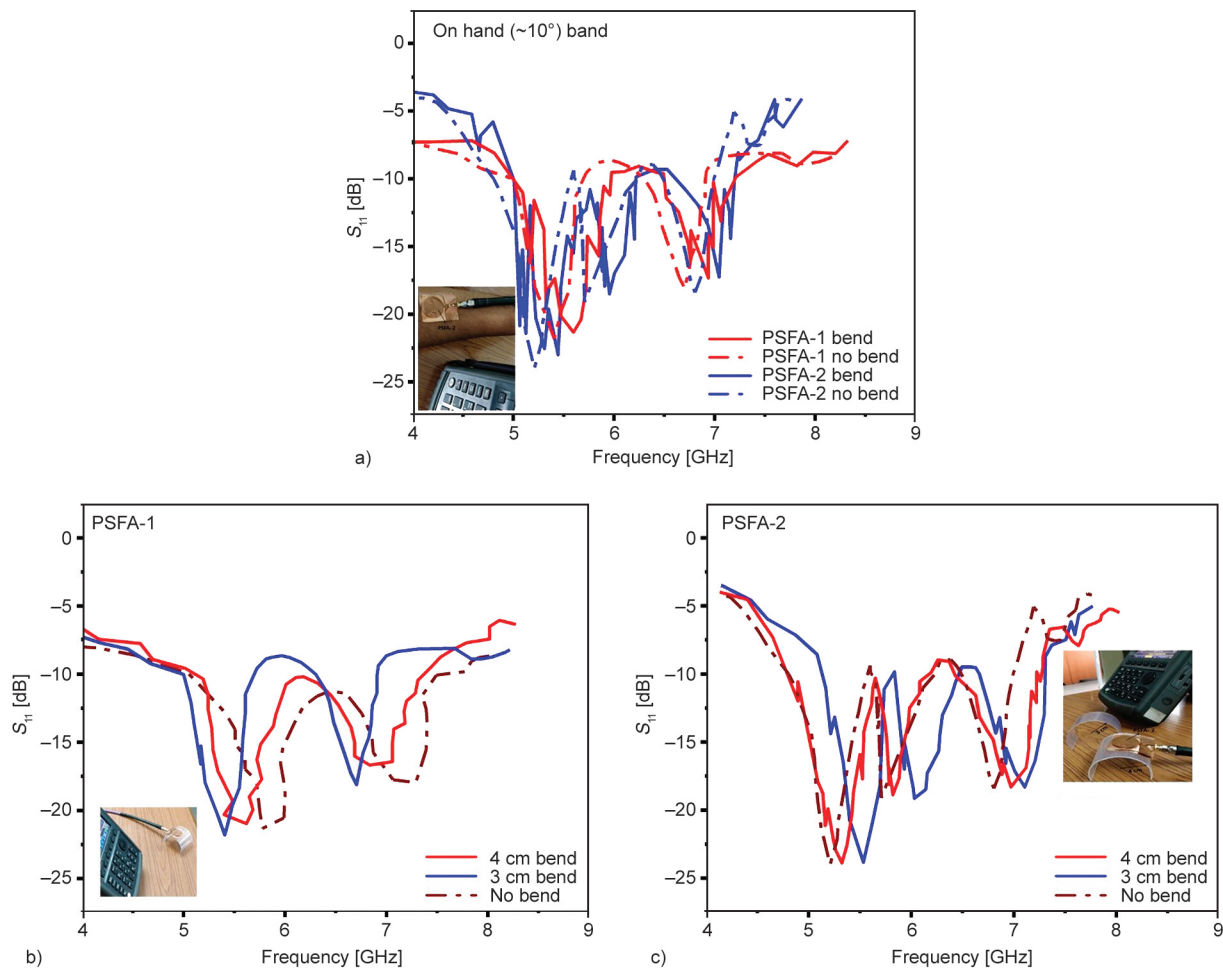


Figure 15.  $S_{11}$  vs. frequency curve: a) on hand; on cylinders of 4.0 and 3.0 cm, b) for PSFA-1, and c) for PSFA-2.

#### 4.4. Wet condition analysis

In the literature, there are several choices for substrates that can be employed to design flexible and wearable antennas. Fabric substrates are the most frequently used substrates for wearable antenna designs. Despite having a variety of benefits, these materials are susceptible to operational environment changes like absorption of moisture and temperature fluctuations that can either directly or indirectly impact the radiation characteristics of the antenna [2]. These constraints have indeed been alleviated by using polymer-based substrates like PDMS, which has been used in this research. This has been demonstrated by evaluating the designed antennas under wet circumstances by submerging them in water, drying them after ten minutes, and evaluating their performance. The analysis presented here demonstrates that flexible antennas built of polymer substrates, such as PDMS, have very little effect from moisture since these materials do not absorb moisture as fabric substrates do. In our earlier study, we compared PDMS with denim substrate [2], where it was shown experimentally that denim is more susceptible to moisture and affects antenna performance more. The measurement setup for the wet condition evaluation and the fluctuation of the  $S_{11}$  parameters in the wet condition is shown in Figure 16. For the proposed antennas using polymer substrate PDMS, very little variation in the resonating frequencies and related  $S_{11}$  parameters is observed. This demonstrates the

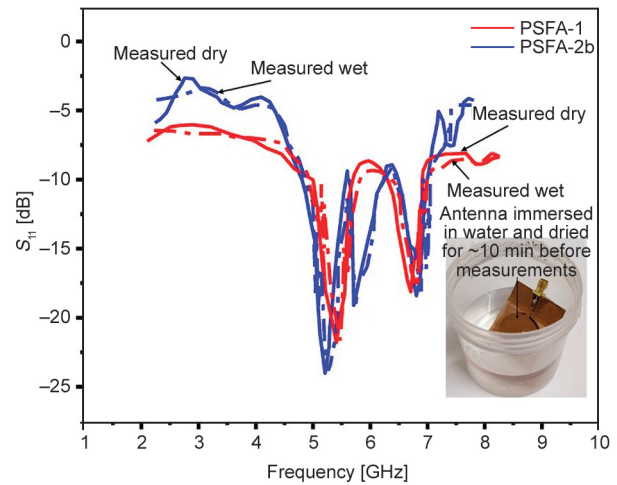


Figure 16. Measured  $S_{11}$  vs. frequency curve for both PSFAs in dry and wet conditions.

PDMS’ appropriateness for the design of flexible antennas with steady performance under a range of operational situations.

#### 5. Conclusions

In this paper, flexible substrate PDMS is employed to design flexible antennas for wireless body and local area network applications. The development and dielectric evaluation of PDMS as per the antenna requirements are also performed here. In order to demonstrate that SRR structures can be employed in flexible antennas with polymer substrates (PSFA) and to experimentally validate the merits of including them in antenna designs, a single CSRR structure is

Table 4. Comparison of PSFA with previous works.

Substrate material	Size [mm <sup>2</sup> ]	Gain [dBi]	Applications	Type of metamaterial loading	Performance analysis in varying operating situations: bending analysis (BA); SAR analysis (SA); on body analysis (OB); wet condition analysis (WA)	References
Polyester	55×46	4.2/5.78	3.63 GHz/4.95 GHz (5G) applications	Not implemented	not performed	[26]
Liquid crystal polymer (LCP)	38×32	2	3.5 GHz (WiMAX)/5.8 GHz (WLAN), applications	Circular SRR (two)	BA	[27]
Polyamide	24×19	2.3/3.3/3.9	2.4 GHz/5.6 GHz (bluetooth), 3.8 GHz (5G NR) applications	Not Implemented	BA; SA; OB	[28]
Polydimethylsiloxane (PDMS)	80×67	4.53	5 GHz/7 GHz (UWB) applications	Not implemented	BA; SA; OB	[29]
Polydimethylsiloxane (PDMS)	70	4.16/4.34	2.45 GHz /5.8 GHz (ISM band) applications	Not implemented	BA; SA; OB	[30]
Polydimethylsiloxane (PDMS)	67×44	6.7	UWB applications	Not implemented	BA; SA; OB	[31]
Polydimethylsiloxane (PDMS)	50.2×40.1	6.2/4.1/2.4	5.12/5.80/6.66 GHz WLAN/WBAN applications	CSRR (single)	BA; SA; OB; WA	Proposed

integrated into the second antenna. It has helped in improving the performance of the PSFA-2, such as an increase in gain from 4.8 to 6.3dBi with better  $V_{SWR}$  and  $S_{11}$  values; the additional frequency band of 5.80 GHz is achieved with 5.12 and 6.66 GHz band in the second antenna for fast wireless body area network applications (Table 4). Reduced SAR and stable performance under different operating situations like bending and wet conditions are the add-on advantages of using CSRR with PDMS. Both of the PSFAs are successfully analyzed for their operability for the target applications due to their simple structure, flexibility, cost-effective development process, and consistent performance under varied operating situations. Prototypes are also fabricated to verify the simulated results that show a good correlation with each other.

### Acknowledgements

This research was supported by Basic Science Research Program through the National Research Foundation of Korea (NRF) funded by the Ministry of Education (NRF-2019R1A6A1A03032119). We would also like to thank Prof (Dr.) Navneet Gupta, Professor and Head, Department of Electrical and Electronics Engineering, Birla Institute of Technology and Science, Pilani, Rajasthan, India for his invaluable support.

### References

- [1] Nguyen T. M., Chung J-Y.: Analysis and fabrication of a wearable antenna using conductive fibers. *Journal of the Korea Academia-Industrial cooperation Society*, **16**, 2770–2776 (2015).  
<https://doi.org/10.5762/KAIS.2015.16.4.2770>
- [2] Sharma P. K., Gupta N.: Design and analysis of polydimethylsiloxane (PDMS) and Jean substrate based flexible antenna for ultra-wideband applications. in ‘Proceeding of 2021 IEEE MTT-S International Microwave and RF Conference (IMARC) Kanpur, India’ 1–4 (2021).  
<https://doi.org/10.1109/IMaRC49196.2021.9714626>
- [3] Zhang K., Soh P. J., Yan S.: Design of a compact dual-band textile antenna based on metasurface. *IEEE Transactions on Biomedical Circuits and Systems*, **16**, 211–221 (2022).  
<https://doi.org/10.1109/TBCAS.2022.3151243>
- [4] Li R., Wu C., Sun X., Zhao Y., Luo W.: An EBG-based triple-band wearable antenna for WBAN applications. *Micromachines*, **13**, 1938 (2022).  
<https://doi.org/10.3390/mi13111938>
- [5] Keshwani V. R., Bhavarthe P. P., Rathod S. S.: Compact embedded dual band EBG structure with low SAR for wearable antenna application. *Progress in Electromagnetics Research M*, **113**, 199–211 (2022).  
<https://doi.org/10.2528/PIERM22071704>
- [6] Sayem A. S. M., Simorangkir R. B. V. B., Esselle K. P., Buckley J. L.: A conformal and transparent frequency reconfigurable water antenna. in ‘Proceedings of 16<sup>th</sup> European Conference on Antennas and Propagation (EuCAP) Madrid, Spain’ 1–4 (2022).  
<https://doi.org/10.23919/EuCAP53622.2022.9769462>
- [7] Shan H., Zhang Y., Gao J., Nag A., Rahaman A.: Integration of different graphene nanostructures with PDMS to form wearable sensors. *Nanomaterials*, **12**, 950 (2022).  
<https://doi.org/10.3390/nano12060950>
- [8] Rojas-Alva U., Møller-Poulsen F., Man S-L., Creamer C., Hanna D., Jomaas G.: Flame spread behaviour of Polydimethylsiloxane (PDMS) membranes in 1 g and  $\mu$ g environments. *Combustion and Flame*, **240**, 112009 (2022).  
<https://doi.org/10.1016/j.combustflame.2022.112009>
- [9] Sharma P. K., Gupta N., Dankov P. I.: Analysis of dielectric properties of polydimethylsiloxane (PDMS) as a flexible substrate for sensors and antenna applications. *IEEE Sensors Journal*, **21**, 19492–19504 (2021).  
<https://doi.org/10.1109/JSEN.2021.3089827>
- [10] Sharma P. K., Gupta N., Dankov P. I.: Characterization of polydimethylsiloxane (PDMS) as a wearable antenna substrate using resonance and planar structure methods. *AEU-International Journal of Electronics and Communications*, **127**, 153455 (2020).  
<https://doi.org/10.1016/j.aeue.2020.153455>
- [11] Sharma P. K., Gupta N., Dankov P. I.: Wideband transmission line characterization of polydimethylsiloxane (PDMS) as a wearable antenna substrate. in ‘Proceeding of IEEE International Conference on Electronics, Computing and Communication Technologies (CONECCT) Bangalore, India’, 1–4 (2020).  
<https://doi.org/10.1109/CONECCT50063.2020.9198526>
- [12] Sharma P. K., Chung J-Y.: Evaluation of polydimethylsiloxane (PDMS) as a substrate for the realization of flexible/wearable antennas and sensors. *Micromachines*, **14**, 735 (2023).  
<https://doi.org/10.3390/mi14040735>
- [13] Gao G-P., Dou Z-H., Yu Z-Q., Zhang B-K., Dong J-H., Hu B.: Dual-mode patch antenna with capacitive coupling structure for on-/off-body applications. *IEEE Antennas and Wireless Propagation Letters*, **21**, 1512–1516 (2022).  
<https://doi.org/10.1109/LAWP.2022.3170555>
- [14] Janapala D. K., Nesasudha M.: A highly miniaturized antenna with wider band for biomedical applications. *Electromagnetic Biology and Medicine*, **41**, 35–43 (2022).  
<https://doi.org/10.1080/15368378.2021.1993892>

- [15] Mukesh A. N., Sharma P. K., Yadav V. P., Payal P. O., Solanki L.: Design and analysis of an edge truncated flexible antenna for wi-fi applications. in 'Proceeding of International Conference on Electronics and Renewable Systems (ICEARS) Tuticorin, India' 1861–1864 (2022).  
<https://doi.org/10.1109/ICEARS53579.2022.9752032>
- [16] Kent G.: Nondestructive permittivity measurement of substrates. *IEEE Transactions on Instrumentation and Measurement*, **45**, 102–106 (1996).  
<https://doi.org/10.1109/19.481319>
- [17] Hasar U. C., Kaya Y., Ozturk H., Izginli M., Ertugrul M., Barroso J. J., Ramahi O. M.: Improved method for permittivity determination of dielectric samples by free-space measurements. *IEEE Transactions on Instrumentation and Measurement*, **71**, 6002108 (2022).  
<https://doi.org/10.1109/TIM.2022.3153991>
- [18] Courtney W. E.: Analysis and evaluation of a method of measuring the complex permittivity and permeability microwave insulators. *IEEE Transactions on Microwave Theory and Techniques*, **18**, 476–485 (1970).  
<https://doi.org/10.1109/TMTT.1970.1127271>
- [19] Kato Y., Horibe M.: Broadband permittivity measurements using a frequency-variable balanced-type circular-disk resonator. in 'Proceeding of 2018 Conference on Precision Electromagnetic Measurements (CPEM 2018) Paris, France' 1–2 (2018).  
<https://doi.org/10.1109/CPEM.2018.8501132>
- [20] Mohammed A. M., Wang Y., Salek M.: Dielectric measurement of substrate materials using 3D printed re-entrant cavity resonator. in 'Proceeding of 51<sup>st</sup> European Microwave Conference (EuMC) London, United Kingdom' 793–796 (2022).  
<https://doi.org/10.23919/EuMC50147.2022.9784354>
- [21] Tiwari N. K., Jha A. K., Singh S. P., Akhter Z., Varshney P. K., Akhtar M. J.: Generalized multimode SIW cavity-based sensor for retrieval of complex permittivity of materials. *IEEE Transactions on Microwave Theory and Techniques*, **66**, 3063–3072 (2018).  
<https://doi.org/10.1109/TMTT.2018.2830332>
- [22] Sharma P. K., Gupta N.: Design and analysis of a compact CSRR loaded defected ground plane antenna for ultra-wideband applications. in 'Proceeding of 2<sup>nd</sup> International Conference on Communication, Computing and Industry 4.0 (C2I4) Bangalore, India' 1–4 (2021).  
<https://doi.org/10.1109/C2I454156.2021.9689449>
- [23] Ali U., Ullah S., Khan J., Kamal B., Basir A., Flint J. A., Seager R. D.: Design and SAR analysis of wearable antenna on various parts of human body, using conventional and artificial ground planes. *Journal of Electrical Engineering and Technology*, **12**, 317–328 (2017).  
<https://doi.org/10.5370/JEET.2017.12.1.317>
- [24] Dankov P. I., Sharma P. K., Gupta N.: Numerical and experimental investigation of the opposite influence of dielectric anisotropy and substrate bending on planar radiators and sensors. *Sensors*, **21**, 16 (2020).  
<https://doi.org/10.3390/s21010016>
- [25] Dankov P. I., Levcheva V. P., Sharma P. K.: Influence of dielectric anisotropy and bending on wearable textile antenna properties. in 'Proceeding of International Workshop on Antenna Technology (iWAT) Bucharest, Romania' 1–4 (2020).  
<https://doi.org/10.1109/iWAT48004.2020.1570606843>
- [26] Afroz S., Al-Hadi A. A., Azemi S. N., Hoon W. F., Padmanathan S., Isa C. M. N. C., Sahoo B. C., Loh Y. S., Suhaimi M. I., Lim L. M., Samsudin Z., Mansor I., Soh P. J.: Dual band circular patch flexible wearable antenna design for sub-6 GHz 5G applications. in 'Proceeding of 2022 IEEE International RF and Microwave Conference (RFM)' Kuala Lumpur, Malaysia, 1–4 (2022).  
<https://doi.org/10.1109/RFM56185.2022.10065238>
- [27] Rao V., Madhav B. T. P., Anilkumar T., Prudhvinadh B.: Circularly polarized flexible antenna on liquid crystal polymer substrate material with metamaterial loading. *Microwave and Optical Technology Letters*, **62**, 866–874 (2020).  
<https://doi.org/10.1002/mop.32088>
- [28] Sreelakshmi K., Rao G. S., Kumar M. N. V. S. S.: A compact grounded asymmetric coplanar strip-fed flexible multiband reconfigurable antenna for wireless applications. *IEEE Access*, **8**, 194497–194507 (2020).  
<https://doi.org/10.1109/ACCESS.2020.3033502>
- [29] Simorangkir R. B. V. B., Kiourti A., Esselle K. P.: UWB wearable antenna with a full ground plane based on PDMS-embedded conductive fabric. *IEEE Antennas and Wireless Propagation Letters*, **17**, 493–496 (2018).  
<https://doi.org/10.1109/LAWP.2018.2797251>
- [30] Simorangkir R. B. V. B., Yang Y., Matekovits L., Esselle K. P.: Dual-band dual-mode textile antenna on PDMS substrate for body-centric communications. *IEEE Antennas and Wireless Propagation Letters*, **16**, 677–680 (2016).  
<https://doi.org/10.1109/LAWP.2016.2598729>
- [31] Janapala D. K., Nesasudha M., Neebha T. M., Kumar R.: Design and development of flexible PDMS antenna for UWB-WBAN applications. *Wireless Personal Communications*, **122**, 3467–3483 (2022).  
<https://doi.org/10.1007/s11277-021-09095-7>